

# Invariance of waveguide grating mirrors to lateral displacement phase shifts

Daniel Brown<sup>1,\*</sup>, Daniel Friedrich<sup>2,\*\*</sup>, Frank Brückner<sup>1</sup>,  
Ludovico Carbone<sup>1</sup>, Roman Schnabel<sup>2</sup> and Andreas Freise<sup>1</sup>

<sup>1</sup>University of Birmingham, School of Physics and Astronomy, Edgbaston, Birmingham, B15 2TT, UK

<sup>2</sup>Institut für Gravitationsphysik, Leibniz Universität Hannover and Max-Planck-Institut für Gravitationsphysik (Albert-Einstein-Institut), Callinstrasse 38, 30167 Hannover, Germany

\*Corresponding author: ddb@star.sr.bham.ac.uk

\*\*Currently working at the Institute for Cosmic Ray Research, University of Tokyo, Japan

Compiled May 2, 2013

We present a method to analyse the coupling of lateral displacements in nanoscale structures, in particular waveguide grating mirrors (WGM), into the phase of a reflected Gaussian beam using a *finite-difference time-domain* simulation. Such phase noise is of interest for using WGMs in high-precision interferometry. We show that, to the precision of our simulations ( $10^{-7}$  rad), waveguide mirrors do not couple lateral displacement into phase noise of a reflected beam and that WGMs are therefore not subject to the same stringent alignment requirements as previously proposed layouts using diffraction gratings. © 2013 Optical Society of America

OCIS codes: 050.2770, 050.5080, 230.4040, 050.1755, 050.6624.

The sensitivity of high precision interferometry experiments such as the preparation of entangled test masses [1], frequency stabilisation with rigid cavities [2] and gravitational wave detectors [3] are eventually limited by the quantum noise of the interrogating light or the thermal noise of the optical components. Quantum shot noise of the detected light can typically be reduced by increasing the laser power. However, this induces larger thermal distortions in the high-reflectivity (HR) coatings and substrates. A number of new techniques have been suggested to reduce the distortions from high power beams as well as thermal noise: the use of non-fundamental beam shapes [4], all-reflective interferometer layouts using dielectric gratings to reduce absorption of the laser in optics [5] and the use of waveguide grating mirrors (WGM) [6]. WGMs would replace HR mirror coatings, reducing their thickness by a factor of 10 to 100; which promises to reduce the Brownian coating thermal noise [3,7]. However, gratings couple lateral displacements into the phase of diffraction orders  $|m| > 0$  [8,9]. This places stringent requirements on the alignment and stability of gratings and the incident laser beams for high-precision interferometry [10]. WGMs rely on diffraction into the first order and could potentially be subject to the same displacement phase noise effects. However, so far no theoretical or experimental evidence has been presented to demonstrate whether WGMs suffer from this.

In this Letter we apply a rigorous *Finite-Difference Time-Domain* (FDTD) based simulation with Gaussian beams to show that WGMs do not couple lateral displacements into the phase of a reflected laser beam. We further provide a simplified ray picture to illustrate this result.

Ray pictures have already been used to describe several WGM features [11] as depicted in Fig.1. WGMs in their most simplistic form consist of 2 layers: (i) a wave-

guide layer applied to some substrate material; and (ii) a grating layer which couples the incident laser light into the waveguide layer (typically etched into the waveguide layer). In this case both the waveguide and grating layers are made from a high refractive index  $n_h$  material with the substrate material's lower refractive index denoted by  $n_l$ . The geometrical grating parameters must be carefully chosen to reach a theoretical maximum reflectivity [6,7]. For given materials and laser light wavelength, the grating period  $d$  is chosen such that the normally incident beam is diffracted into the 1<sup>st</sup> order within the waveguide layer at an angle that allows total-internal-reflection (TIR) at the waveguide-substrate boundary to occur. TIR at the substrate boundary along with the grating create a waveguide in which the  $\pm 1^{\text{st}}$  orders propagate. These undergo diffraction at the grating multiple times, coupling out into the vacuum where it interferes with the reflected specular laser light. The remaining grating parameters, namely the thickness of the waveguide layer  $s$ , fill-factor  $f$  and groove depth  $g$  can all be tuned to provide destructive interference in the substrate and constructive in the vacuum, ideally providing 100% reflectivity.

A lateral displacement  $\delta x$  of some grating structure versus the incident beam induces a phase shift of

$$\Delta\Phi_m = 2\pi m\delta x/d \quad (1)$$

relative to a non-displaced beam for diffraction order  $m$  [10]. For WGMs we require that any rays coupling out into the vacuum do not have any phase terms dependent on  $\delta x$ . From Fig.1 each time a ray is diffracted and picks up a  $\Delta\Phi_m$  term, an \* is added as a superscript. The ray  $-1T^{**}$  diffracted into the vacuum has collected two  $\Delta\Phi_m$  terms, its total phase is then  $\Phi_{-1T^{**}} = \Phi_o(s, d, g, f, n_l, n_h) + \Delta\Phi_{+1} + \Delta\Phi_{-1}$ , where  $\Phi_o$  is a collection of all phase terms depending on the WGM

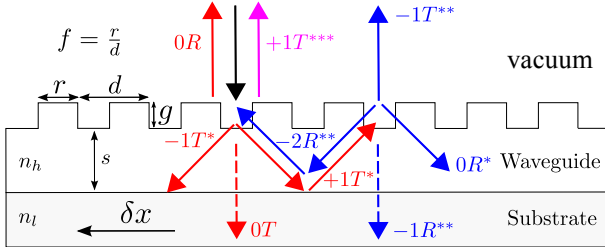


Fig. 1. The incident beam (black) is coupled into the waveguide layer by the grating into  $m = \pm 1$ . Orders  $\pm 1T$  propagate along the waveguide coupling back into the vacuum (blue) to interfere with the initially reflected light,  $0R$ , picking up  $\Delta\Phi_m$  phase terms with each interaction with the grating. Further coupling into the vacuum is also possible (magenta) which involved further  $\Delta\Phi_m$  terms. The \* superscript refers to the number of diffractions beam has undergone.  $R$  = Reflection from grating,  $T$  = Transmission from grating, first number is order of diffraction  $m$ .

parameters, but not  $\delta x$ .  $\Phi_0$  is tuned with simulations by adjusting each parameter to produce 100% reflectivity. From Eq.(1) we see the  $\Delta\Phi_{-1}$  and  $\Delta\Phi_{+1}$  terms cancel, with a similar argument being valid for all other rays that couple out into the vacuum such as  $+1T^{***}$ . Thus, following this strongly simplified picture any of the phase noise effects outlined in Ref. [10] for gratings should not apply to WGMs under normal incidence.

In order to provide a rigorous and physically correct computer model of a finite beam reflected from a WGM we have implemented a numerical finite-difference time-domain (FDTD) based algorithm, which provides the ability to model a variety of grating structures as well as arbitrary and finite incident electromagnetic field distributions. The simulation tool is coded in *Java*, open sourced (<http://kvasir.sr.bham.ac.uk/redmine/projects/fdtd>) and was based on Ref. [12]. A 2D FDTD simulation sufficed for our needs as only a displacement of the WGM in one direction orthogonal to a normally incident Hermite-Gaussian (HG) beam was required; thus speeding up computation time significantly. Two extra features were also required for the simulation [12]: *Total-Field Scattered-Field* (TFSF) for separating the incident and reflected beam from the WGM and *complex perfectly matched layers* (CPML) to reduce reflections from the simulation boundaries. The simulation package was validated by reproducing known dependencies (found in Ref. [6]) of the reflectivity as a function of the grating parameters and by investigating the phase noise of standard diffraction gratings [9].

The aim of the simulation was to measure the wavefront of a HG beam reflected from a WGM whilst displacing it from  $\delta x = 0 \rightarrow d$ . Along the wavefront the phase can then be deduced and plotted against  $\delta x$  to view any apparent phase shifts. The simulation setup is depicted in Fig.2, where a HG  $\text{TEM}_{00}$  is injected in the  $\hat{x}$  direction along the TFSF boundary and the elec-

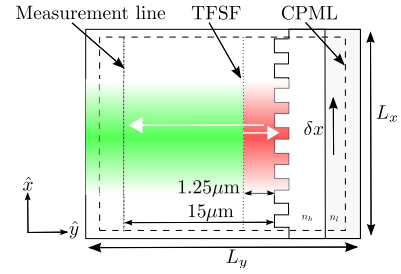


Fig. 2. Schematic layout of 2D FDTD simulation for testing WGM shift invariance. Gaussian beam injected along TFSF boundary onto WGM (Red). The reflected beam (Green) then propagates to the measurement line where the phase is measured. The CPML absorbs outgoing waves to reduce reflections from boundaries.

tric field of the reflected beam is measured along the measurement line  $15\mu\text{m}$  away to avoid near-field variations. The *Courrant stability factor* [12] for the simulation was chosen as  $S = c\Delta t/\Delta x = 1/\sqrt{2}$ ; where  $\Delta t$  is the simulation timestep and  $\Delta x = \Delta y = 25\text{nm}$  are the size of the 2D discretisation of the simulation space with dimensions  $L_y = 250\Delta y$  and  $L_x = 4000\Delta x$ . The injected beam had a wavelength  $\lambda = 1064\text{nm}$  and was positioned such that the waist was at the WGM with size  $w_0 = 800\Delta x = 20\mu\text{m}$ . The WGM parameters chosen were  $d = 28\Delta x = 700\text{nm}$ ,  $g = 14\Delta x = 350\text{nm}$ ,  $f = 0.5$  and  $s = 5\Delta x = 125\text{nm}$  which provided a reflectivity of 99.8% for the incident beam (in agreement with Ref. [6]). The indices of refraction used were fused silica for  $n_l = 1.45$  and  $\text{Ta}_2\text{O}_5$  for  $n_h = 2.084$  which are the typical materials used for 1064nm optics.

Eq.1 states the phase shift for  $m = \pm 1$  is periodic with displacements of the grating period  $d = 28\Delta x$ . Thus for this effect to be visible the simulation was run 28 times for offsets  $\delta x = p\Delta x$  with  $p = 0, 1, 2, \dots, 28$ . Approximately 3000 timesteps were required for the reflected beam to reach an approximate steady-state in each simulation. At this point 1024 time samples of the electric field at each point along the measurement line were taken,  $E_p(x, t)$ . The generalised Goertzel algorithm (based on Fast Fourier Transforms (FFT)) [13] was used to extract the amplitude  $A_p(x)$  and phase  $\phi_p(x)$  of the reflected beam along the measurement line for the incident laser frequency  $f_0 = c/1064\text{nm}$ .  $\phi_p(x)$  was obtained for each offset  $\delta x = p\Delta x$  of the WGM with the change in phase with displacement defined as  $\Delta\phi_p(x) = \phi_p(x) - \phi_0(x)$ . Our model showed that displacement phase shift for WGMs are at least  $10^5$  smaller than for an equivalent grating setup, see Fig.3: The central plot shows the phase change as a function of the displacement along the beam profile; the satellite plots provide the scale for the central plot. The top plot shows  $\Delta\phi_{14}$  increasing slightly towards the edge of the beam, this is expected to occur when  $A_p(x) \rightarrow 0$ , which degrades any accurate calculation of the phase as the *signal-to-numerical noise* ratio decreases. At the beam peak, shown in the

right plot, the phase change is  $\Delta\phi_p(x=0) \approx 20\mu\text{rad}$  and shows no correlation with  $\delta x$ . This result is 5 orders of magnitude smaller than what Eq.(1) states for displaced grating structures. To determine whether the oscillations seen in  $\Delta\phi_p(x)$  were near field effects or numerical artefacts the value  $\max\{\Delta\phi_p(x)\}$  was computed at increasing distances from the WGM for a displacement over one grating period  $p = 0 \rightarrow 28$  at the centre of the beam ( $x = -d/2 \rightarrow d/2$ ). As seen in Fig.4, the near field phase shifts from the initial imprint of the grating can be seen at  $y < 3\mu\text{m}$  which decays rapidly with distance, after which a flat noise is present. Fig.4 shows 3 different FFT windowing functions agreeing at  $y < 3\mu\text{m}$  but possessing different noise floors, the lowest being  $\max\{\Delta\phi_p(x)\} \approx 10^{-7}\text{rad}$  using a *Blackman* FFT window. Numerical errors present from the FDTD are not thought to be limiting, increased spatial and temporal resolution ( $\Delta x \rightarrow \Delta x/2$ ) does not offer any improvement in the noise levels as seen in Fig.4. This suggests *spectral leakage* from the FFT is limiting the accuracy of phase measurements and the oscillations present in  $\Delta\phi_p(x)$  measured at  $15\mu\text{m}$  are purely numerical artefacts, similar results were seen at varying distances from the WGM.

This work presents the successful implementation of an FDTD simulation to analyse displacement induced phase shifts in a reflected Gaussian beam from a WGM. No such phase shifts were found within the precision limit of  $\approx 10^{-7}\text{rad}$  set by numerical errors. This lower limit is seven orders of magnitude lower than the phase noise estimated for previously proposed layouts with diffraction gratings, which raised concerns regarding the stability and alignment [10] of such configurations. Therefore, the absence of this phase shift for WGMs strengthens the argument for their usage in future high-precision interferometry experiments.

We acknowledge the Science and Technology Facilities Council (STFC) for financial support in the UK. D.F. was supported by the Deutsche Forschungsgemeinschaft (DFG) within the Collaborative Research Centre TR7. This document has been assigned the LIGO Laboratory Document number ligo-p1300019.

## References

1. H. Müller-Ebhardt, H. Rehbein, R. Schnabel, K. Danzmann, and Y. Chen, *Phys. Rev. Lett.* **100**, 013601 (2008)
2. K. Numata, A. Kemery, and J. Camp, *Phys. Rev. Lett.* **93**, 250602 (2004)
3. G. M. Harry, A. M. Gretarsson, P. R. Saulson, S. E. Kittelberger, S. D. Penn, W. J. Startin, S. Rowan, M. M. Fejer, D. R. M. Crooks, G. Cagnoli, J. Hough, and N. Nakagawa, *CQG* **19**, 897 (2002)
4. S. Chelkowski, S. Hild, and A. Freise, *Phys. Rev. D* **79**, 122002 (2009)
5. K.-X. Sun and R. L. Byer, *Opt. Lett.* **23**, 567 (1998)
6. A. Bunkowski, O. Burmeister, D. Friedrich, K. Danzmann, and R. Schnabel, *CQG* **23**, 7297 (2006)
7. F. Brückner, T. Clausnitzer, O. Burmeister,

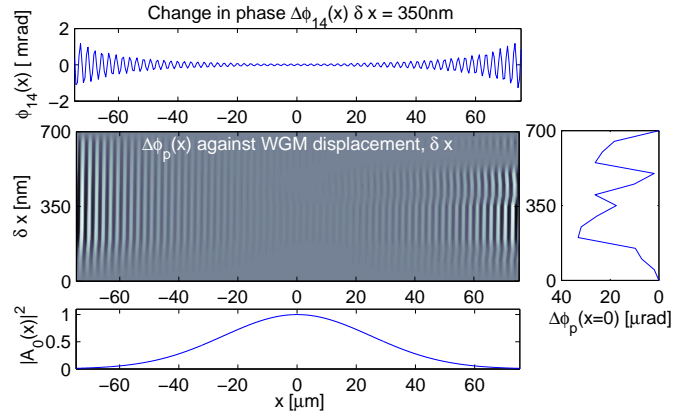


Fig. 3. Central plot shows phase change in the reflected beams wavefront  $\Delta\phi_p(x)$  against WGM displacement,  $\delta x$ . Top plot shows cross section of phase at  $\delta x = 350\text{nm}$  where the phase change is maximum. The right plot shows the variation in the phase of at  $x = 0$  against  $\delta x$ . Bottom plot shows the intensity of the reflected beam along  $x$ .

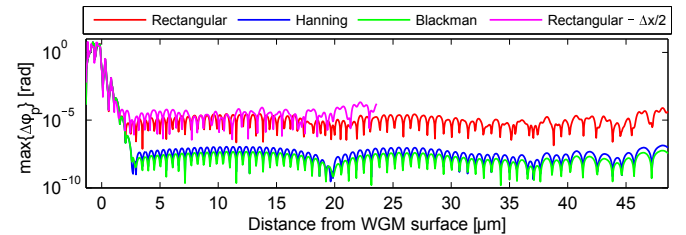


Fig. 4. Maximum change in phase at beam peak intensity as the WGM is displaced from  $\delta x = 0 \rightarrow d$  with increasing distance from the WGM surface and different FFT windowing functions. Large near field phase shifts are seen close to the WGM and then a flat noise. Increasing the spatial and temporal resolution of FDTD  $\Delta x \rightarrow \Delta x/2$  did not appear to offer reductions in numerical noise caused by FDTD.

8. D. Friedrich, E.-B. Kley, K. Danzmann, A. Tünnermann, and R. Schnabel, *Opt. Lett.* **33**, 264 (2008)
8. S. Wise, V. Quetschke, A. J. Deshpande, G. Mueller, D. H. Reitze, D. B. Tanner, B. F. Whiting, Y. Chen, A. Tünnermann, E. Kley, and T. Clausnitzer, *Phys. Rev. Lett.* **95**, 013901 (2005)
9. D. Lodhia, D. Brown, F. Brückner, and A. Freise, in preparation (2013)
10. A. Freise, A. Bunkowski, and R. Schnabel, *New Journal of Physics* **9**, 433 (2007)
11. A. Sharon, D. Rosenblatt, and A. A. Friesem, *J. Opt. Soc. Am. A* **14**, 2985 (1997)
12. A. Taflove and S. C. Hagness, *Computational Electrodynamics: The Finite-Difference Time-Domain Method* 3rd ed. (Artech House Publishers, 2005)
13. P. Sysel and P. Rajmic, *EURASIP Journal on Advances in Signal Processing* **2012**, 1 (2012). 10.1186/1687-6180-2012-56